International Research Journal of Advanced Engineering and Science
ISSN (Online): 2455-9024

Fluid Flow, Heat and Mass Transfer Analysis of MHD Nanofluid Over a Non-Linear, Variable Temperature Surface

A. Falana, J.O. Oyediran
Department of Mechanical Engineering, University of Ibadan, Ibadan, Nigeria
Email: falanaayode@gmail.com, ojoyediran64@gmail.com

Abstract*— *In this study, we investigate the effects of mass, heat, and fluid flow over a stretching sheet that is of variable temperature surface. We looked into how skin friction and other parameters affected the rate of heat transfer in a nanofluid over which the cooling takes place. Using similarity variable functions, the governing partial differential equations (PDEs) for continuity, momentum, energy, and concentration of nanoparticles are converted to ordinary differential equations (ODEs). The Runge-Kutta Fehlberg method is utilized to solve the equations numerically. The results showed that the local Nusselt number $(-\theta')$ for Pr =1, n =0.2 for Cortell is 0.610262, Bhargava et al is 0.6113, Zaimi et al is 0.61131 respectively and for the present work is 0.61131 showing that the results are in close agreement.

***Keywords*— *Stretching sheet, boundary layer, magnetic effect, similarity transformation, nanofluids*.**

I. INTRODUCTION

This This work, which has several industrial implications, aims to analyze the rate of heat transfer in a MHD nanofluid flow across a non-linear, non-isothermal stretched sheet using. The thermal characteristics of boundary layer flow on a stretching sheet (Tsou et al., 1967). Since then, a number of studies on the boundary layer of continuously moving surfaces have been conducted. Heat transfer and flow properties on stretched and moving surfaces were explored (Crane 1970), (Gupta et al., 1977), (Soundalgekar et al., 1980), (Grubka et al., 1985). However, they limited their investigation to the study of flow characteristics and heat transmission in the absence of a magnetic field. The magnetic parameter has an equal impact to the viscoelastic parameter after examining the behavior of a viscoelastic MHD fluid over a stretched sheet (Andersson, 1992).

A form of fluid known as nanofluid is created by dispersing nanoparticles into a base fluid with low thermal conductivity, like water or ethylene glycol, to boost the fluid's thermal conductivity. More heat may be transferred out of the cooling chamber to these particles, which are often made of metal or metal oxide and improve conduction and convection coefficients (Choi, 1995). It appears that several researchers embraced the term "nanofluid," which was initially used by Choi and Eastman. Materials with nanoscale diameters have special chemical and physical properties. Because they are small enough to behave like liquid molecules, they can pass through micro channels without clogging them. Due to the small size of the nano elements and the low volume fraction of nano elements needed for conductivity enhancement, they are also very stable and do not have any extra issues like sedimentation, erosion, addition pressure drops, or nano-Newtonian behavior (Choi et al., 1995).

Numerous significant technical applications in the fields of metallurgy and chemical processes are related to the flow over a stretching sheet. Among many applications, we have continuous strips or filaments drawn through a quiescent fluid to cool them. The research of constant two-dimensional boundary layer flow of Newtonian fluid over stretching surfaces (Crane, 1970).

Extrusion is a crucial step in the production process in many industries. The rate at which heat transfers from the stretching sheets determines the quality of the product. Thermal radiation and magnetohydrodynamics' influence on convective heat transfer are crucial to the phenomena of electrically conducting fluid flowing past a heated surface and to high-temperature thermal processes like those found in nuclear power plants and power generators. These effects on boundary layer flow across an increasingly stretching sheet (Swati, 2013).

The results for the temperature profile, concentration profile, local Nusselt number (heat transfer), and Sherwood number (mass transfer) for different values of Prandtl number *Pr*, magnetic parameter κ, Brownian effect *Nb*, thermophoresis effect *Nt*, and Lewis number *Le* are provided. When the current results are compared to established numerical results, they are discovered to be close in agreement (Falana et al., 2014), (Chandrasekar et al., 2015), (Falana,2022).

II. METHODOLOGY

2.1 Formulation of the Problem

Here, we are looking at a continuous, two-dimensional, electrically conducting flow of a nanofluid with velocity u and v in the x *and* $y-$direction over a non-linear, non-isothermal stretching sheet. It is assumed that the stretching surface velocity, $u = ax^n$, where n is an exponent and a is a constant. Since the induced magnetic field is so little in comparison to the applied magnetic field, it can be disregarded. The following are the governing equations:

$$\frac{\partial u}{\partial x} + \frac{\partial v}{\partial y} = 0 \quad (1)$$

$$u\frac{\partial u}{\partial x} + v\frac{\partial v}{\partial y} = v\frac{\partial^2 u}{\partial y^2} - \frac{\kappa {B_0}^2}{\rho_f}u \quad (2)$$

A. Falana, J.O. Oyediran, "Fluid Flow, Heat and Mass Transfer Analysis of MHD Nanofluid Over a Non-Linear, Variable Temperature Surface," *International Research Journal of Advanced Engineering and Science*, Volume 11, Issue 2, pp. 40-44, 2026.

International Research Journal of Advanced Engineering and Science
ISSN (Online): 2455-9024

$$u\frac{\partial T}{\partial x} + v\frac{\partial T}{\partial y} = \alpha\left(\frac{\partial^2 T}{\partial y^2}\right) + \tau\left[D_B\left(\frac{\partial C}{\partial y}\frac{\partial T}{\partial y}\right) + \frac{D_T}{T_\infty}\left(\frac{\partial T}{\partial y}\right)^2\right] \quad (3)$$

Figure 1 illustrates how a rise in the dimensionless velocity profile (f') is a result of an increase in the nonlinear stretching rate (n). Figure 2 illustrates how, when other parameters remain constant, an increase in the nonlinear stretching rate (n) results in an increase in the dimensionless skin friction (f'').

At a point $\eta = 0.2$, Figure 3 illustrates how an increase in the thermophoresis parameter *(Nt)* decreases the temperature profile (θ). Figure 4 illustrates how a decrease in heat transfer rate $-\theta'$ results from an increase in the thermophoresis parameter *(Nt)* when other parameters are constant. Figure 5 illustrates how, when other parameters remain constant, an increase in the thermophoresis parameter *(Nt)* leads to a rise in concentration (ϕ).

As the thermophoresis parameter *(Nt)* increases, Figure 6 illustrates how mass transfer rate $-\phi'$ increases at $\eta = 0.3$ and thereafter decreases.

Figure 7 shows that increase in Brownian motion parameter *(Nb)* causes decrease in temperature (θ). Figure 8 shows that increase in Brownian motion parameter *(Nb)* causes decrease in heat transfer (reduced Nusselt number) $-\theta'$ when other parameters are constant. Figure 9 shows that increase in Brownian motion parameter *(Nb)* causes decrease in concentration profile (ϕ).

In Figure 10, increase in Brownian motion parameter *(Nb)* causes rise in mass transfer (reduced Sherwood number) $-\phi'$ at a point $\eta = 0.3$ and later falls when other parameters are fixed.

$$y \to 0 \Rightarrow u = U_0 = ax, v = 0, T = T_0 = T_\infty + Ax^n, C = C_0 \quad (4)$$

$$y \to \infty \Rightarrow u = 0, v = 0, T = T_\infty, C = C_\infty \quad (5)$$

where T, C, v, and u stand for the fluid's temperature, concentration, transverse direction, and longitudinal velocity, respectively. The kinematic viscosity, electrical conductivity, externally imposed magnetic field in the y-direction, fluid density, Brownian diffusion coefficient, thermophoresis diffusion coefficient, and temperature of the stretched sheet are represented by the symbols υ, κ, B_0, $\rho_f, D_B, D_T, and\ T_0$ respectively. It is presumable that the sheet's temperature T_0 is higher than the surrounding air temperature T_∞. where 'a' is the stretched sheet's typical length. The dimensionless similarity variables are as follows:

$$\eta = x^{\frac{n-1}{2}} y\sqrt{\frac{a(n+1)}{2\upsilon}}, u = ax^n f'(\eta), \theta(\eta) = \frac{T - T_\infty}{T_0 - T_\infty}$$

$$v = -\sqrt{\frac{a\upsilon(n+1)}{2}} x^{\frac{n-1}{2}} + \left(f(\eta) + \left(\frac{n-1}{n+1}\right)\eta f'(\eta)\right), \phi(\eta) = \frac{C - C_\infty}{C_0 - C_\infty}$$

The stream function (ψ) is applied and therefore the continuity equation (1) is completely satisfied as $u = \frac{\partial \psi}{\partial y}, v = -\frac{\partial \psi}{\partial x}$.

The final ordinary differential equations (ODEs) are as follows after transformations:

$$f''' + ff'' - \frac{2n(f')^2}{n+1} - M \quad (6)$$

$$\frac{1}{Pr}\theta'' + N_b\phi'\theta' + N_t(\theta')^2 + f\theta' = 0 \quad (7)$$

$$\phi'' + \frac{N_t}{N_b}\theta'' + Lef\phi' = 0 \quad (8)$$

Such that,

$$y \to 0, \quad f = 0,\ f' = 1,\ \theta = 1,\ \phi = 1$$
$$y \to \infty,\ f = 0,\ f' = 0,\ \theta = 0,\ \phi = 0 \quad (9)$$

The parameters of interest Pr, M, Nb, Nt and Le. The Prandtl number is represented by $Pr = \frac{\upsilon}{\alpha}$, the magnetic parameter by $M = \frac{\kappa {B_0}^2}{\rho_f a}$, the Brownian motion parameter by $N_b = \frac{\tau D_B (C_0 - C_\infty)}{\upsilon}$, the thermophoresis parameter by $N_t = \frac{\tau D_T (T_0 - T_\infty)}{\upsilon T_\infty}$ and the Lewis number by $Le = \frac{\upsilon}{D_B}$. The physical quantities of skin friction (shear stress), heat transfer (Nusselt number), and mass transfer (Sherwood number) are derived as follows [16;

Skin friction formular (shear stress):

$$C_f = \frac{\tau_w}{\rho(U_w)^2} = \frac{\mu\frac{\partial u}{\partial y}}{\rho(U_w)^2} = {Re_x}^{-1/2}\sqrt{\frac{n+1}{2}} f''(0)$$

$$C_f = {Re_x}^{-1/2}\sqrt{\frac{n+1}{2}} f''(0) \quad (10)$$

The following formula yields the local heat transfer rate (also known as the local Nusselt number):

$$Nu_x = \frac{xq_w}{k(T_w - T_\infty)} = -\left(\frac{Re_x v}{a}\right)^{\frac{1}{2}}\sqrt{\frac{a(n+1)}{2v}}\theta'(0)$$

$$Nu_x {Re_x}^{-1/2} = -\sqrt{\frac{(n+1)}{2}}\theta'(0) \quad (11)$$

The Sherwood local number is;

$$Sh_x = \frac{xq_m}{D_B(C_w - C_\infty)} = -\left(\frac{Re_x v}{a}\right)^{\frac{1}{2}}\sqrt{\frac{a(n+1)}{2v}}\phi'(0)$$

$$Sh_x {Re_x}^{-1/2} = -\sqrt{\frac{(n+1)}{2}}\phi'(0) \quad (12)$$

where the symbols for the mass flux rates and the wall heat flux respectively, are $q_m\ and\ q_w$.

III. RESULTS AND DISCUSSION

The Runge-Kutta Fehlberg fourth and fifth order approach is utilized to numerically integrate equations (6) - (8) for various parameter values, including the thermophoresis parameter, Lewis numbers, magnetic parameter, and Prandtl. We examine how the emerging parameters affect the rates of heat and mass transfer, temperature, skin friction, and dimensionless velocity. Using a value of 2 for η_{max}, the asymptotic boundary conditions in Equation (9) were estimated as follows.

$$\eta_{max} = 2;\ f'(2) = \theta(2) = \phi(2) = 0$$

This guarantees the accurate approach of numerical solutions to the asymptotic values. In order to verify the current

A. Falana, J.O. Oyediran, "Fluid Flow, Heat and Mass Transfer Analysis of MHD Nanofluid Over a Non-Linear, Variable Temperature Surface," *International Research Journal of Advanced Engineering and Science*, Volume 11, Issue 2, pp. 40-44, 2026.

International Research Journal of Advanced Engineering and Science
ISSN (Online): 2455-9024

solution, a comparative analysis was conducted between Table 1 and 2 $-\theta'(0)$ and $-\phi'(0)$ data with previously published literature data. The results demonstrated a high degree of closeness. Table 3 displays the effects of magnetic parameters on the skin friction, Nusselt, and Sherwood numbers while maintaining fixed values for the stated parameters. Tables 1-3 demonstrate that the Nusselt number decreases as a function of M, n, Nt, and Le, while the Sherwood number decreases as a function of M, n, and Nt and increases as a function of Pr and Le. We observed that a higher Lewis number would slow down heat transfer. Table 3 shows that the values of the skin friction coefficient increase with different values of M.

TABLE 1: Comparison of $-\theta'(0)$ for Pr and n values when Nb =Nt =M = 0.

Pr	n	Cortell 2007	Bhargava et al., 2012	Zaimi et al., 2014	Present Results
1	0.2	0.610262	0.6113	0.61131	0.61131
	0.5	0.395277	0.5967	0.59668	0.59668
	1.5	0.574537	0.5768	0.57686	0.57686
	2.0	-	-	0.57245	0.57245
	3.0	0.564472	0.5672	0.56719	0.56719
	4.0	-	-	0.56415	0.56415
	10.0	0.554960	0.5578	0.55783	0.55783
5	0.2	1.607175	1.5910	1.60757	1.60757
	0.5	1.586744	1.5839	1.58658	1.58658
	1.0	-	-	1.56787	1.56787
	1.5	1.557463	1.5496	1.55751	1.55751
	2.0	-	-	1.55093	1.55093
	3.0	1.542337	1.5372	1.54271	1.54271
	10	1.528573	1.5260	1.52877	1.52877

TABLE 2: Nusselt and Sherwood values compared when Pr =Le =2 and M= 0.

n	Nt	Nb	Bhargava et al., 2012		Present results	
			$-\theta'(0)$	$-\phi'(0)$	$-\theta'(0)$	$-\phi'(0)$
0.2	0.1	0.5	0.5160	0.9012	0.5148	0.9014
	0.3		0.4533	0.8395	0.4520	0.8402
	0.5		0.3999	0.8048	0.3987	0.8059
3.0	0.1		0.4864	0.8445	0.4852	0.8447
	0.3		0.4282	0.7785	0.4271	0.7791
	0.5		0.3786	0.7379	0.3775	0.7390
10.0	0.1		0.4799	0.8323	0.4788	0.8325
	0.3		0.4227	0.7654	0.4216	0.7660
	0.5		0.3739	0.7238	0.3728	0.7248

TABLE 3: Skin friction coefficient, Sherwood number, and Nusselt calculations for a range of M values for Pr =6.2; Le = 5; Nb = Nt = 0.1 and n =2

M	$f''(0)$	$-\theta'(0)$	$-\phi'(0)$
0	1.10102	1.06719	1.07719
0.5	1.30989	1.04365	1.01090
1	1.48912	1.02337	0.95495

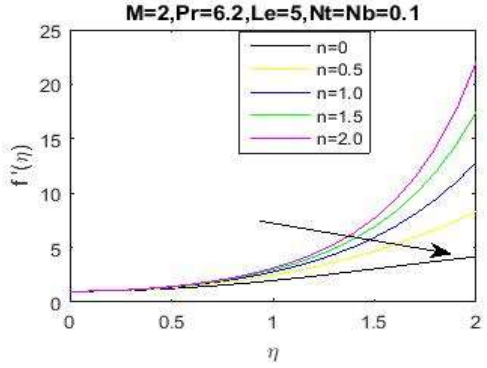

Figure 1: n effects on dimensionless velocity profile

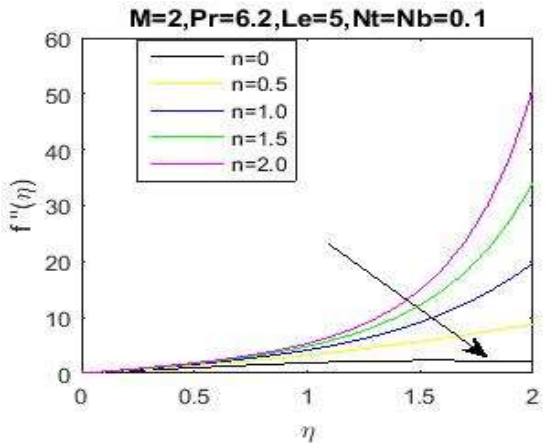

Figure 2: n effects on dimensionless skin friction

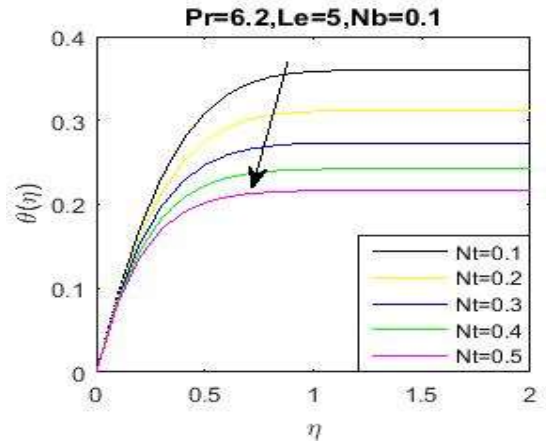

Figure 3: Thermophoresis' effects on dimensionless temperature

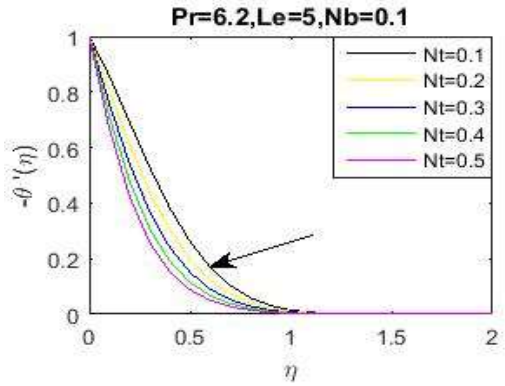

Figure 4: Thermophoresis' effects on dimensionless heat transfer

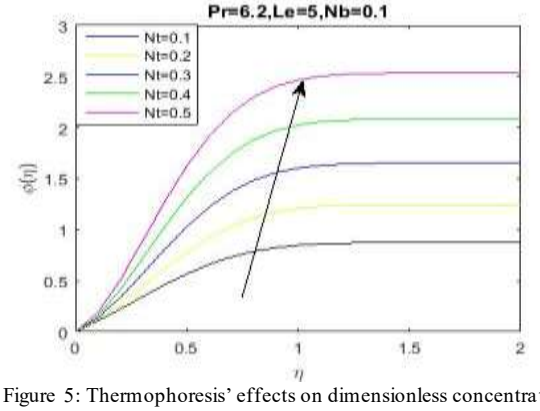

Figure 5: Thermophoresis' effects on dimensionless concentration

A. Falana, J.O. Oyediran, "Fluid Flow, Heat and Mass Transfer Analysis of MHD Nanofluid Over a Non-Linear, Variable Temperature Surface," *International Research Journal of Advanced Engineering and Science*, Volume 11, Issue 2, pp. 40-44, 2026.

International Research Journal of Advanced Engineering and Science
ISSN (Online): 2455-9024

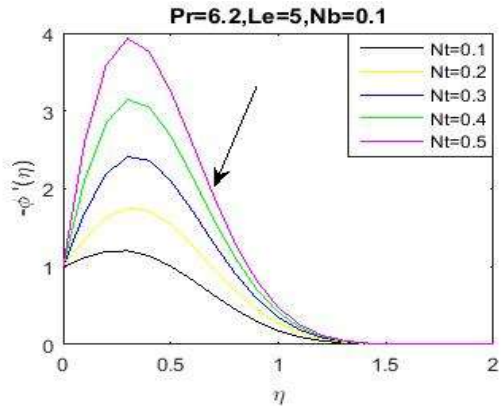

Figure 6: Thermophoresis' effects on dimensionless mass transfer

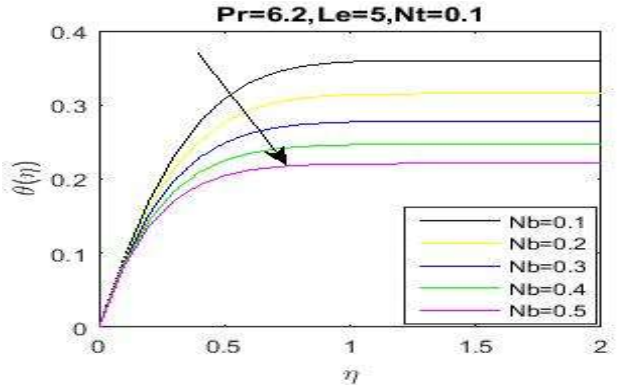

Figure 7: Brownian motion effects on dimensionless temperature

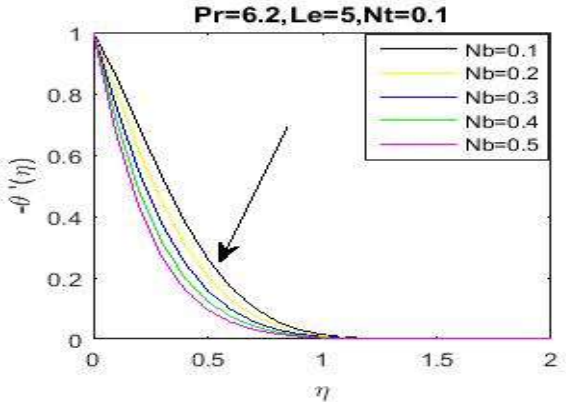

Figure 8: Brownian motion effects on dimensionless heat transfer

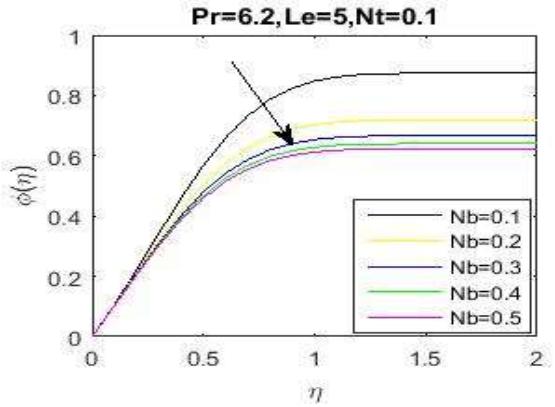

Figure 9: Brownian motion effects on dimensionless concentration

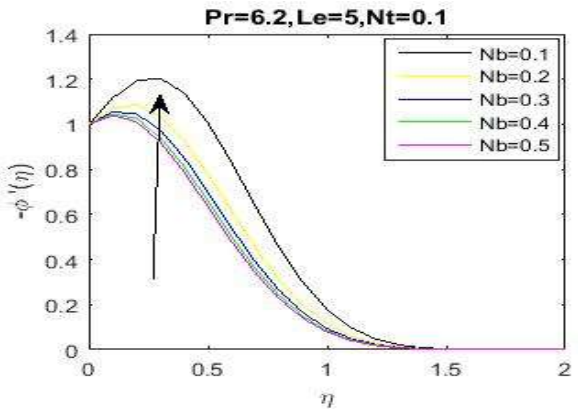

Figure 10: Brownian motion effects on dimensionless mass transfer

Figure 1 illustrates how a rise in the dimensionless velocity profile (f') is a result of an increase in the nonlinear stretching rate (n). Figure 2 illustrates how, when other parameters remain constant, an increase in the nonlinear stretching rate (n) results in an increase in the dimensionless skin friction (f'').

At a point $\eta = 0.2$, Figure 3 illustrates how an increase in the thermophoresis parameter *(Nt)* decreases the temperature profile (θ). Figure 4 illustrates how a decrease in heat transfer rate $-\theta'$ results from an increase in the thermophoresis parameter *(Nt)* when other parameters are constant. Figure 5 illustrates how, when other parameters remain constant, an increase in the thermophoresis parameter *(Nt)* leads to a rise in concentration (ϕ).

As the thermophoresis parameter *(Nt)* increases, Figure 6 illustrates how mass transfer rate $-\phi'$ increases at $\eta = 0.3$ and thereafter decreases.

Figure 7 shows that increase in Brownian motion parameter *(Nb)* causes decrease in temperature (θ). Figure 8 shows that increase in Brownian motion parameter *(Nb)* causes decrease in heat transfer (reduced Nusselt number) $-\theta'$ when other parameters are constant. Figure 9 shows that increase in Brownian motion parameter *(Nb)* causes decrease in concentration profile (ϕ).

In Figure 10, increase in Brownian motion parameter *(Nb)* causes rise in mass transfer (reduced Sherwood number) $-\phi'$ at a point $\eta = 0.3$ and later falls when other parameters are fixed.

IV. CONCLUSION

A numerical investigation has been conducted into the MHD boundary layer flow and heat transfer of a nanofluid over a nonlinear stretching sheet and a variable temperature surface. A similarity solution with Runge-Kutta Fehlberg fourth and fifth order was used. Both quantitative and graphical presentations of the impact of the governing parameters on the flow, concentration, and heat transfer characteristics are obtained. The following are the primary findings of the current investigation:

- Velocity profile and skin friction increases with the nonlinear stretching parameter.
- Rate of heat transfer decreases whereas there is a slight increase in mass transfer with an increase in both thermophoresis and Brownian motion parameters.

A. Falana, J.O. Oyediran, "Fluid Flow, Heat and Mass Transfer Analysis of MHD Nanofluid Over a Non-Linear, Variable Temperature Surface," *International Research Journal of Advanced Engineering and Science*, Volume 11, Issue 2, pp. 40-44, 2026.

- The values of the skin friction coefficient increase with different values of *M*.

REFERENCES

[1]. Int. J. Heat and Mass Transf. 10 (1967) 219-235; F.K. Tsou, E.M. Sparrow, R.J. Goldstein, Flow and Heat transfer in the boundary layer on a continuous moving surface.
[2]. L.J. Crane, "Flow through an elastic band," Mathematics and Physics, Z. 21, 1970, 645–647. Heat and mass transfer on a stretching sheet with suction or blowing, P.S. Gupta, A.S. Gupta, 55 (1977) 744-746 in Can. J. Chem. Eng.
[3]. Warme Stoffubert, 14 (1980) 91-93; V.M. Soundalgekar, T.V.R. Murthy, Heat transfer in the flow past a continuous moving plate with varying temperature.
[4]. ASME J. Heat Transf. 107 (1985) 248-250; L.J. Grubka, K.M. Bobba, Heat transfer characteristics of a continuous stretched surface with changeable temperature.
[5]. Acta Mech. 95 (1992) 227-230; H.I. Andersson, MHD flow of a viscoelastic fluid via a stretched surface.
[6]. U.S. Choi, Advancements and uses of non-Newtonian flows: augmenting fluids' thermal conductivity with nanoparticles, ASME. FED.231/MD.66 (1995) 99-105, eds. D.A. Siginer and H.P. Wang.
[7]. The paper "Enhancing thermal conductivity of fluids with nanoparticles" was published in the Proceedings of the ASME International Mechanical Engineering Congress and Exposition in November 1995. It was written by U.S. Choi and J.A. Eastman and covered pages 12–17.
[8]. Flow past a stretching plate, L.J. Crane, J. Appl. Math. Phys. 21 (1970) 645–647.
[9]. Apl. Math. Comput. 184 (2007) 864–873, R. Cortell, Viscous flow and heat transport over a nonlinearly extending sheet.
[10]. R. Bhargava, P. Rana, and Commun. Nonlinear Sci. Numer. Simul 17 (2012) 212–226. Flow and heat transport of a nanofluid over a nonlinearly stretching sheet: a numerical investigation.
[11]. M. Swati, slip effects on MHD boundary layer flow between heat radiation and suction/blowing over an exponentially stretched sheet Eng. J. Ain Shams 4 (2013) 485–491.
[12]. Boundary layer flow and heat transfer over a nonlinearly permeable stretching/shrinking sheet in a nanofluid, K. Zaimi, A. Ishak, and I. Pop, Sci. Rep. 4 (2014) 4404. 10.1038/srep04404 at http://dx.doi.org.
[13]. Falana and R.O. Fagbenle (2014). Forced convection thermal boundary layer transfer for non-isothermal surfaces using modified merk series. Open journal of Fluid Dynamics, 4, pp. 241 - 250
[14]. Magneto hydrodynamic flow with viscous dissipation effects in the presence of injection and suction, M. Chandrasekar, M.S. Kasiviswanathan, 93-107 in J. Theor. Appl. Mech. 53 (2015).
[15]. Falana, Analysis of Fluid Flow and Heat Transfer over a Non-isothermal Inclined Flat Plate using the Modified Merk Series of Chao and Fagbenle. Nigerian Research Journal of Engineering and Environmental Sciences 7(1) 2022 pp. 384-392. http://doi.org/10.5281/zenodo.6726595.